

Spontaneous rotation in one-dimensional systems of cold atoms

Akiyuki Tokuno^{1,2} and Masahiro Sato³

¹*Department of Physics, Tokyo Institute of Technology,
Oh-okayama, Meguro-ku, Tokyo 152-8551, Japan*

²*Institute for Solid State Physics, University of Tokyo, Kashiwa 227-8581, Japan*

³*Condensed Matter Theory Laboratory, RIKEN, Wako, Saitama 351-0198, Japan*

(Dated: February 9, 2022)

We theoretically study harmonically trapped one-dimensional Bose gases (e.g., ⁷Li, ²³Na, ³⁹K, ⁸⁷Rb, etc.) with multibands occupied, focusing on effects of higher-energy bands. Combining the Ginzburg-Landau theory with the bosonization techniques, we predict that the repulsive interaction between higher-band bosons and the quantum fluctuation can induce the ground state with a finite angular momentum around the trapped axis. In this state, the Z_2 reflection symmetry (clockwise or anticlockwise rotations) is spontaneously broken.

PACS numbers: 05.30.Jp, 03.75.Hh

I. INTRODUCTION

For the last decade, cold-atom systems [1, 2, 3, 4] have been vigorously studied and experimental techniques of controlling them have been greatly developed. As a result, we can now tune various parameters of cold-atom systems, even including dimensionality. These developments have enabled us to encounter several phenomena: For instance, superfluid-insulator transitions on optical lattices, dynamics of Bose-Einstein condensations (BECs), BCS-BEC crossover in Fermi gases, etc. They are all difficult to be realized within traditional experiments using electronic systems in solids.

Among various new fields of cold-atom physics, in this paper, we focus on one-dimensional (1D) trapped Bose gases [5, 6, 7, 8, 9]: For example, polarized atoms ⁷Li, ²³Na, ³⁹K, ⁸⁷Rb, etc. One-dimensional quantum systems have been shown to exhibit unusual interesting features due mainly to effects of strong quantum fluctuations. For example, it is widely known that BECs never occur even at zero temperature in 1D repulsively interacting Bose gases in the thermodynamic limit. Instead, a Tomonaga-Luttinger liquid (TLL) state is predicted to appear. Actually TLL and Tonks-Girardeau (TG) gas [10] – the hard-core interacting limit of TLL – behaviors have been observed in recent experiments of 1D cold Bose gases. [11, 12]

One-dimensional confined systems in cold-atom experiments often take a cigar shape as shown in Fig. 1. This shape is of course caused by a 2D (y - z plane) potential, which strongly restricts the in-plane dynamics and makes the radial energy spectrum discrete, i.e., yields a multi-band structure. The dimensionality of the cigar-shaped systems is known to be determined by the 3D s -wave scattering length a between atoms and the particle density ρ per 1D unit length. For $a\rho \ll 1$ the system may be regarded as a purely 1D gas, namely, almost all of the atoms are in the lowest band. On the other hand, for the opposite case $a\rho \gg 1$, 3D nature strongly survives. In the former case, the low-energy physics is characterized by a single dimensionless parameter $\gamma^{-1} = a_{1D}\rho$,

where a_{1D} is the effective 1D scattering length. [8] A small γ corresponds to the weakly interacting regime in which low-energy properties can be captured by mean-field (Gross-Pitaevskii-type) theory, whereas for a large γ , effects of the interaction is considerably strong and thus the TLL or TG-gas behaviors clearly emerge.

Thanks to the recent studies of purely 1D atomic gases, their understanding has been greatly deepened. However, there still exist important issues in 1D confined systems: One of them is what happens if atoms occupy not only lowest band but also higher ones. As yet, effects of higher bands have not been well discussed well. Since multi bands may be regarded as an internal degrees of freedom such as electron spins, the system is expected to contain rich physical properties. In this paper, we will provide an answer to this problem. To this end, we consider a simple 3D single-component Bose gas system with a repulsive interaction and a 2D harmonic potential. As we will explain, due to the potential, each energy band takes an angular momentum l : the lowest band has $l = 0$, the second lowest ones have $l = \pm 1$ and are hence doubly degenerate, and so on. A positive (negative) l corresponds to atoms rotating clockwise (anticlockwise) around the confinement axis. For simplicity, we will concentrate on the case where only the lowest band and the degenerate

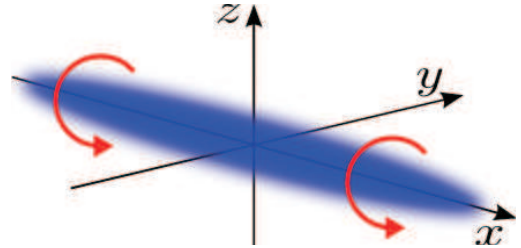


FIG. 1: One-dimensional trapped Bose gas confined along the x axis. In the text, we predict that the Bose gas spontaneously circulates along the arrow (or along the opposite direction of the arrow) under a certain condition.

second lowest ones (totally three bands) are occupied. In this situation, it is shown that at least if the 2D harmonic potential is sufficiently stronger than the interaction between atoms, the particle densities of the $l = \pm 1$ bands become imbalanced and the ground state spontaneously rotates with a finite angular momentum as shown in Fig. 1. We will explain in detail the mechanism of this spontaneous rotation phenomenon.

This paper is organized as follows. First, we define the 3D Hamiltonian of the Bose atoms confined by a 2D harmonic potential in Sec. II. Then, we reduce the 3D Hamiltonian to the 1D effective one in order to describe the low-energy physics. In Secs. III and IV, based on the reduced Hamiltonian, we analyze the low-energy physics of the trapped bosons. Employing the Ginzburg-Landau (GL) theory and the bosonization techniques, we show that the spontaneous rotation as in Fig. 1 can occur under certain, realistic conditions. The final Section V is devoted to the summary and the discussions for our results. In Appendix A, we summarize the symmetries of our Bose gas system, which play important roles in the analyses of Secs. III and IV.

II. BOSE GAS AND EFFECTIVE HAMILTONIAN

First, we introduce a 3D Bose gas in the presence of a 2D harmonic potential, whose Hamiltonian is defined as

$$H = \int d\vec{r} \left[\psi^\dagger \left(-\frac{\hbar^2 \nabla^2}{2m} - \mu + V(\vec{r}) \right) \psi + \frac{U}{2} \mathcal{D}^2 + \dots \right], \quad (1)$$

where $\psi(\vec{r})$ and $\mathcal{D} = \psi^\dagger \psi$ are the annihilation field and the density operator of the bosons, respectively. Positive parameters m , μ and U respectively mean the mass of bosons, the chemical potential and the repulsive coupling constant. The 3D s-wave scattering length a is related to U via $U = 4\pi\hbar^2 a/m$. Three or more-body interactions are assumed to be quite small compared with U . The 2D confinement potential V is a harmonic type: $V(\vec{r}) = \frac{1}{2}m\omega_0^2(y^2 + z^2) - \hbar\omega_0$, where the axial direction is equal to the x axis (see Fig. 1). Here we note that the Hamiltonian (1) is invariant under the Z_2 reflection and the SO(2) rotation in the $y-z$ plane [$\psi(x, y, z) \rightarrow \psi(x, -y, z)$ and $\psi(\vec{r}) \rightarrow \psi(x, y \cos \Phi - z \sin \Phi, y \sin \Phi + z \cos \Phi)$, where $\Phi \in \mathbf{R}$]. Other symmetries of the model (1) are discussed in Appendix A.

In order to make the one dimensionality of the model (1) more visible, it is useful to expand $\psi(\vec{r})$ in terms of eigenstates of the 2D harmonic oscillator $u_{n,l}(y, z)$ as follows:

$$\psi(\vec{r}) = \sum_{n=0}^{\infty} \sum_l u_{n,l}(y, z) \phi_{n,l}(x), \quad (2)$$

where l is the angular momentum in the $y-z$ plane and can take $-n, -n+2, \dots, n-2, n$ for a given n . The angular momentum is a good quantum number because of the

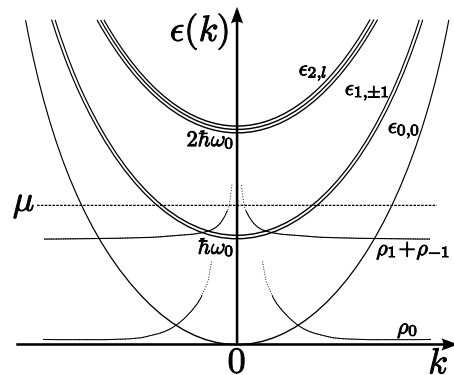


FIG. 2: Single-particle energy band structure and density distributions (sketch) in each band. We assume that the bosons live only in lower three energy bands. The density ρ_α is defined in Eq. (6).

SO(2) rotational symmetry of Eq. (1). The boson field $\phi_{n,l}$ describes the physics of the x direction. Substituting Eq. (2) into Eq. (1), we obtain the single-particle energy dispersion $\epsilon_{n,l}(k) = \frac{\hbar^2 k^2}{2m} + \hbar\omega_0 n$ which is shown in Fig. 2. It is noteworthy that all of the bands $\epsilon_{n,l}$ with the same index n are degenerate, i.e., the $(n+1)$ -fold degeneracy exists. For example, as we already mentioned, the second lowest bands $\epsilon_{1,\pm 1}$ are doubly degenerate.

To discuss effects of multi bands, we assume that the bosons occupy the lower three bands $\epsilon_{0,0}$, $\epsilon_{1,\pm 1}$ as in Fig. 2. To satisfy this situation, we impose the following conditions:

$$\hbar\omega_0 < \mu < 2\hbar\omega_0, \quad (3)$$

$$a/a_\perp \ll 1 \quad (\text{i.e., } \hbar\omega_0 \gg U/a_\perp^3), \quad (4)$$

$$2\hbar\omega_0 - \mu \gg U/a_\perp^3, \quad (5)$$

where the confinement radius $a_\perp = \sqrt{\hbar/m\omega_0}$ represents the width of the wave function $u_{n,l}(y, z)$ around the origin $(y, z) = (0, 0)$. The first condition (3) ensures that the lower three bands have finite boson densities. The other ones (4) and (5) mean that the energy scale between neighboring bands is sufficiently larger than the strength of the interaction. These would allow us to neglect bosons in all of the higher bands $\epsilon_{n>2,l}$ (i.e., bands $\epsilon_{n>2,l}$ are nearly empty of bosons).

Under these assumptions, let us continue to study the model (1). Since the low-energy physics must be governed by the bosons on occupied bands with $(n, l) = (0, 0), (1, \pm 1)$, the low-energy effective theory can be obtained by integrating out the degrees of freedom of the bosons on all the vacant bands. In order to carry out this integration, it is convenient to introduce the Euclidean action corresponding to the Hamiltonian (1) through the

path integral formalism as $S_{\text{tot}} = S_0 + S_1 + S_{\text{int}}$,

$$S_0 = \int d\tau dx \sum_{n=0}^1 \sum_l \phi_{n,l}^* \left[\partial_\tau - \frac{\hbar}{2m} \partial_x^2 - \mu + n\hbar\omega_0 \right] \phi_{n,l} \\ + \frac{U}{8\pi a_\perp} \left[2\rho_{0,0}^2 + \rho_{1,1}^2 + \rho_{1,-1}^2 + 4\rho_{0,0}(\rho_{1,1} + \rho_{1,-1}) \right. \\ \left. + 4\rho_{1,1}\rho_{1,-1} + 2(\phi_{0,0}^* \phi_{0,0}^* \phi_{1,1} \phi_{1,-1} + h.c.) \right], \quad (6a)$$

$$S_1 = \int d\tau dx \sum_{n=2}^{\infty} \sum_l \phi_{n,l}^\dagger \left[\partial_\tau - \frac{\hbar}{2m} \partial_x^2 - \mu + n\hbar\omega_0 \right] \phi_{n,l}, \quad (6b)$$

$$S_{\text{int}} = \frac{U}{2} \int d\tau dx \sum'_{\{n_i\}} \sum'_{\{l_i\}} P_{l_1, l_2, l_3, l_4}^{n_1, n_2, n_3, n_4} \\ \times \phi_{n_1, l_1}^* \phi_{n_2, l_2}^* \phi_{n_3, l_3} \phi_{n_4, l_4}, \quad (6c)$$

where τ is the imaginary time, and $\rho_{n,l} = \phi_{n,l}^* \phi_{n,l}$ is a boson density of a band (n, l) . The prime of the summations in S_{int} means the sum over all the possible sets of (n_i, l_i) ($i = 1, \dots, 4$) except for all of the interaction terms of S_0 . Equations (6a) and (6b) are, respectively, the part including only the bosons of the occupied bands and the kinetic part of massive bosons of all the empty bands. The remaining part S_{int} contains all the interaction terms including empty-band boson fields. The coupling constants $P_{l_1, l_2, l_3, l_4}^{n_1, n_2, n_3, n_4}$ in S_{int} are expressed as

$$P_{l_1, l_2, l_3, l_4}^{n_1, n_2, n_3, n_4} = \int dy dz u_{n_1, l_1}^* u_{n_2, l_2}^* u_{n_3, l_3} u_{n_4, l_4}. \quad (7)$$

The integration of the empty-band bosons in S_{tot} can be performed by making use of the representations (6a)-(6c) and the cumulant expansion. The resulting action is written as $S_{1D} = S_0 + \langle S_{\text{int}} \rangle_1 - \frac{1}{2} (\langle S_{\text{int}}^2 \rangle_1 - \langle S_{\text{int}} \rangle_1^2) + \dots$, where $\langle \dots \rangle_1$ stands for the expectation value with respect to S_1 . For the action S_{1D} , effects of higher-energy bands are taken into account through virtual scattering processes. In this calculation process, the Matsubara Green's function $G_n(\tau, x) = -\langle T_\tau \phi_{n,l}(x, \tau) \phi_{n,l}^*(0, 0) \rangle$ of the massive bosons with $\epsilon_{n>2,l}$ may be approximated as $\lambda_n^{-1} \Theta_s(\tau) \Theta_s(\lambda_n - |x|) \Theta_s(\Delta_n - |\tau|)$, where $\lambda_n = \sqrt{2\pi\hbar^2/m\Delta_n}$ is the thermal de Broglie wave length, $\Delta_n = n\hbar\omega_0 - \mu$ is the gap of bosons, and Θ_s is the Heaviside's step function.

The resulting effective Hamiltonian corresponding to the action S_{1D} is given as

$$H_{1D} = \int dx \mathcal{H}_0 + \mathcal{H}_{\text{int}}, \quad (8a)$$

$$\mathcal{H}_0 = \frac{\hbar^2}{2m} \sum_\alpha \partial_x \phi_\alpha^\dagger \partial_x \phi_\alpha - \mu_0 \rho_0 - \mu_1 (\rho_1 + \rho_{-1}), \quad (8b)$$

$$\mathcal{H}_{\text{int}} = \frac{U}{8\pi a_\perp^2} \left[2\Gamma_0 \rho_0^2 + \Gamma_1 (\rho_1^2 + \rho_{-1}^2) + 4\Gamma_{01} \rho_0 (\rho_1 + \rho_{-1}) \right. \\ \left. + 4\Gamma_{\pm 1} \rho_1 \rho_{-1} + 2\Gamma_{0\pm 1} (\phi_0^\dagger \phi_0^\dagger \phi_1 \phi_{-1} + h.c.) \right], \quad (8c)$$

where $\alpha = 0, \pm 1$ correspond to band indices $(n, l) = (0, 0), (1, \pm 1)$, respectively. The Hamiltonian \mathcal{H}_0 is the free boson part and $\mu_0 = \mu > 0$ and $\mu_1 = \mu - \hbar\omega_0 > 0$ are the chemical potentials. The first and second terms in \mathcal{H}_{int} are the two-body interactions in the same band. The third and fourth are those between the different bands. The final term is the tunneling between the lowest band and the doubly degenerate bands. The coupling constants Γ_α are modified from unity (the bare value in S_0) due to vacant-band effects.

Calculating lower-order cumulants carefully, one can find that, for example, massive bosons on $\epsilon_{2,l}$ varies coupling constants as $\Gamma_\alpha \approx 1 + \sum_{n=1}^{\infty} c_{\alpha,n} (a/a_\perp)^n$ ($c_{\alpha,n}$ are nonuniversal constants). This result strongly supports that the cumulant expansion is reliable and works out under the conditions (3)-(5) and $\Gamma_\alpha = 1$ is semi-quantitatively correct. The cumulant expansion generates other three- or more-body interactions, but they are also negligible compared with the two-body ones in \mathcal{H}_{int} .

III. ANALYSIS I

In the preceding section, we have obtained the 1D effective Hamiltonian (8). Here, analyzing it, let us investigate the low-energy properties of the Bose gas under the conditions (3)-(5). First, to evaluate the mean density profile of each band, we introduce the following GL potential from \mathcal{H}_{int} ,

$$\mathcal{F}_{\text{GL}} = -\mu_0 \rho_0 - \mu_1 \rho_s + \frac{U}{8\pi a_\perp^2} \left[2\Gamma_0 \rho_0^2 + \Gamma_s \rho_s^2 + \Gamma_a \rho_a^2 \right. \\ \left. + 4\Gamma_{01} \rho_0 \rho_s + 2\Gamma_{0\pm 1} \rho_0 \sqrt{\rho_s^2 - \rho_a^2} \cos(2\theta_0 - 2\theta_s) \right], \quad (9)$$

where $\Gamma_{s,a} = (\Gamma_1 \pm 2\Gamma_{\pm 1})/2$ and we have defined $\phi_\alpha = \rho_\alpha^{1/2} e^{i\theta_\alpha}$, $\rho_{s,a} = \rho_1 \pm \rho_{-1}$ and $\theta_{s,a} = (\theta_1 \pm \theta_{-1})/2$. The quantity ρ_s is the total density in the second lowest bands, while ρ_a stands for the angular momentum density in the same bands [the total angular momentum is $\mathcal{L} = \sum_{n,l} \int dx l \rho_{n,l}(x)$]. Therefore, a solution with $\rho_a \neq 0$, if possible, means the emergence of the spontaneous rotation and the breakdown of the Z_2 reflection symmetry in the trapped plane. Each term in \mathcal{F}_{GL} has the following physical meanings: (i) Positive $\mu_{0,1}$ induce finite densities $\rho_{0,\pm 1} \neq 0$ and the relation $\mu_0 \gg \mu_1$ must yield $\rho_0 \gg \rho_{\pm 1}$, (ii) $\Gamma_{0,s} (> 0)$ tend to decrease $\rho_{0,s}$, while $\Gamma_a (< 0)$ promotes the growth of ρ_a , (iii) $\Gamma_{01} (> 0)$ favors the decrease of $\rho_{0,s}$, and (iv) the tunneling $\Gamma_{0\pm 1} (> 0)$ inversely enhances $\rho_{0,s}$ and decreases ρ_a . Recalling the condition (4), we can guess that bosons on the second lowest bands interact only with the lowest-band bosons with a kinetic energy $\epsilon_{0,0}(k) \sim \hbar\omega_0$, and hardly influence the bosons with lower energies. It is hence expected that Γ_{01} and $\Gamma_{0\pm 1}$ are overestimated in \mathcal{F}_{GL} . Here, we simply regard both the density amplitude ρ_α and the phase θ_α as c numbers, although for real quantum systems, we cannot fix them simultaneously. This approximation would also overestimate the effects of $\Gamma_{0\pm 1}$.

The GL equations $\partial\mathcal{F}_{\text{GL}}/\partial\rho_\alpha = \partial\mathcal{F}_{\text{GL}}/\partial\theta_\alpha = 0$ are solved as

$$\bar{\rho}_0 = \frac{4\pi a_\perp^2}{U} \frac{\Gamma_s \mu_0 - (2\Gamma_{01} - 2\Gamma_{0\pm 1})\mu_1}{2\Gamma_0 \Gamma_s - (2\Gamma_{01} - \Gamma_{0\pm 1})^2}, \quad (10a)$$

$$\bar{\rho}_s = \frac{4\pi a_\perp^2}{U} \frac{-(2\Gamma_{01} - \Gamma_{0\pm 1})\mu_0 + 2\Gamma_0 \mu_1}{2\Gamma_0 \Gamma_s - (2\Gamma_{01} - \Gamma_{0\pm 1})^2}, \quad (10b)$$

$$\bar{\rho}_a = 0, \quad (10c)$$

$$\bar{\theta}_0 - \bar{\theta}_s = \pi/2. \quad (10d)$$

Furthermore, computing $\partial^2\mathcal{F}_{\text{GL}}/\partial\rho_\alpha\partial\rho_\beta$, we find that the above solution is stable and minimize \mathcal{F}_{GL} . Because of $\bar{\rho}_a = 0$, the GL argument shows no symmetry breaking. If we straightforwardly adopt the approximation $\Gamma_\alpha = 1$, $\bar{\rho}_s$ becomes negative under the condition (3). This is unphysical and attributed to large Γ_{01} and $\Gamma_{0\pm 1}$, as expected. To recover a physical solution $\bar{\rho}_0 > \bar{\rho}_s \neq 0$, we should replace Γ_{01} and $\Gamma_{0\pm 1}$ with small values, $\tilde{\Gamma}_{01}$ and $\tilde{\Gamma}_{0\pm 1}$, respectively: For example, when we set $\tilde{\Gamma}_{01} = \tilde{\Gamma}_{0\pm 1} = a/a_\perp \ll 1$, the GL equations offer a reasonable solution $\bar{\rho}_s \approx \frac{8\pi a_\perp^2}{3U} (\mu_1 - \frac{a}{2a_\perp} \mu_0)$.

Let us next take into account the quantum fluctuation around the physical GL solution. To this end, the bosonization [9, 13, 14] is powerful and unbiased. It makes the density and field operators transform as

$$\rho_\alpha \approx \left(\bar{\rho}_\alpha + \frac{1}{\pi} \partial_x \varphi_\alpha \right) \sum_{n=-\infty}^{\infty} e^{i2n(\varphi_\alpha - \pi \bar{\rho}_\alpha x)}, \quad (11a)$$

$$\phi_\alpha \approx \sqrt{\bar{\rho}_\alpha + \frac{1}{\pi} \partial_x \varphi_\alpha} \sum_{n=-\infty}^{\infty} e^{i2n(\varphi_\alpha - \pi \bar{\rho}_\alpha x)} e^{-i(\bar{\theta}_\alpha + \theta_\alpha)}, \quad (11b)$$

where the phase fields θ_α and $\varphi_{\alpha'}$ ($\alpha, \alpha' = 0, \pm 1$) represent the quantum fluctuation and obey $[\theta_\alpha(x), \partial_{x'} \varphi_{\alpha'}(x')] = [\varphi_\alpha(x), \partial_{x'} \theta_{\alpha'}(x')] = i\pi \delta_{\alpha, \alpha'} \delta(x - x')$. Here we define $\varphi_{s,a} = \varphi_1 \pm \varphi_{-1}$. Substituting the formula (11) into Eq. (8), we obtain the phase-field Hamiltonian, which is invariant under the symmetry operations (A1) and (A2). Remarkably, due to $\Gamma_a < 0$, the coefficient of $(\partial_x \varphi_a)^2$ becomes negative in the Hamiltonian. This means that the (φ_a, θ_a) sector has an instability against the fluctuation of ρ_a . It might be restored by sufficiently large higher-order differential terms such as $(\partial_x \varphi_a)^4$ [15], but the emergence of those terms would not be expected under the condition (4). We thus conclude that the quantum fluctuation violates the GL solution and induces a ground state with a finite angular momentum $\bar{\rho}_a \neq 0$. It is known that similar scenarios of symmetry breakings can occurs in a few systems. [15, 16, 17, 18]

IV. ANALYSIS II

In order to examine and to enhance the validity of the above prediction of $\bar{\rho}_a \neq 0$, let us reconsider the effective theory (8) using another approximation. As we already

mentioned, Γ_{01} and $\Gamma_{0\pm 1}$ terms are expected to be overestimated in Eq. (9). Therefore, at first we daringly drop the tunneling term with $\Gamma_{0\pm 1}$ and replace Γ_{01} with a small effective value $\tilde{\Gamma}_{01}$. For this simplified case, the GL potential is written as

$$\begin{aligned} \tilde{\mathcal{F}}_{\text{GL}} = & -\mu_0 \rho_0 - \mu_1 \rho_s + \frac{U}{8\pi a_\perp^2} [2\Gamma_0 \rho_0^2 + \Gamma_s \rho_s^2 \\ & + \Gamma_a \rho_a^2 + 4\tilde{\Gamma}_{01} \rho_0 \rho_s]. \end{aligned} \quad (12)$$

The GL equations $\partial\tilde{\mathcal{F}}_{\text{GL}}/\partial\rho_\alpha = 0$ lead to $\bar{\rho}_0 = \frac{2\pi a_\perp^2}{U} \frac{\Gamma_s \mu_0 - 2\tilde{\Gamma}_{01} \mu_1}{\Gamma_0 \Gamma_s - 2\tilde{\Gamma}_{01}}$, $\bar{\rho}_s = \frac{4\pi a_\perp^2}{U} \frac{\Gamma_0 \mu_1 - \tilde{\Gamma}_{01} \mu_0}{\Gamma_0 \Gamma_s - 2\tilde{\Gamma}_{01}}$ and $\bar{\rho}_a = 0$. Namely, the GL solution again suggests no angular momentum. However, considering the stability of the solution, we see that the density profile $(\bar{\rho}_0, \bar{\rho}_s, \bar{\rho}_a)$ corresponds to the saddle point for $\tilde{\mathcal{F}}_{\text{GL}}$ and it is minimized at $\rho_a \rightarrow \pm\infty$ which is unphysical. The reason for this instability is that the interband interaction $\Gamma_{\pm 1}$ is stronger than intraband one Γ_1 . To recover a physically proper solution, we can add the following phenomenological term $\frac{U}{8\pi a_\perp^2} \frac{\Gamma_a^{(4)}}{4} \rho_a^4$ ($\Gamma_a^{(4)} > 0$) to $\tilde{\mathcal{F}}_{\text{GL}}$. [19] It is interpreted that this term originates from the higher-order corrections of the cumulant expansion or many-body interactions neglected in the original Hamiltonian (1). This modification offers a stable, physical solution

$$\bar{\rho}_a = \pm \sqrt{-\frac{2\Gamma_a}{\Gamma_a^{(4)}}}. \quad (13)$$

From the consideration above, we see that the GL approach with neglecting the tunneling term naturally leads to a finite angular momentum.

As in the previous analysis in Sec. III, let us bosonize the Hamiltonian (8) based on the GL solution (13). At this stage, we recover the tunneling term. The resulting phase-field Hamiltonian is represented as

$$\begin{aligned} \mathcal{H}_{1D} \approx & \int dx \sum_{\alpha=0,s,a} \frac{v_\alpha}{2\pi} \{ K_\alpha (\partial_x \theta_\alpha)^2 + K_\alpha^{-1} (\partial_x \varphi_\alpha)^2 \} \\ & + \tilde{g}_{sa} \partial_x \theta_s \partial_x \theta_a + \tilde{g}_{0s} \partial_x \varphi_0 \partial_x \varphi_s \\ & + \tilde{g} \cos(2\theta_0 - 2\theta_s) + \dots \end{aligned} \quad (14)$$

Coefficients of $(\partial_x \theta_0)^2$, $(\partial_x \theta_s)^2$ and $(\partial_x \theta_a)^2$ are proportional to $\bar{\rho}_0$, $\bar{\rho}_s$ and $\bar{\rho}_a$, respectively, while $\tilde{g}_{sa} \propto \bar{\rho}_a$.

Therefore, when $\bar{\rho}_a$ is smaller enough than $\bar{\rho}_{0,s}$, any instability of restoring $\bar{\rho}_a = 0$ does not originate from the differential terms. In addition, the symmetry operations (A2) indicate that any vertex term with φ_a or θ_a is forbidden in the Hamiltonian (14). [18] Thus, we can say that $\bar{\rho}_a \neq 0$ is not destroyed by the quantum fluctuation and it agrees with our previous approach in Sec. III. The symmetries also tell us that for all of the vertex operators, only $\cos[2n(\theta_0 - \theta_s)]$ ($n \in \mathbf{Z}$) are allowed to appear in the phase-field Hamiltonian. The final term of Eq. (14) is the most relevant in the allowed vertex interactions. Generally, for 1D boson systems with repulsive short-range

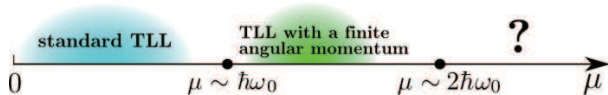


FIG. 3: Predicted ground-state phase diagram of the model (1) under the condition (4). Quantum phase transitions are expected to occur around the black points. They, however, might be interrupted as a crossover phenomenon rather than a transition, since boson densities of higher bands would be nonzero even when the chemical potential μ is smaller than $\hbar\omega_0$. When μ is larger than $n\hbar\omega_0$ ($n > 2$), the bosons on higher bands $\epsilon_{n>2,l}$ would also possess an angular momentum. It is therefore expected that, for example, the bosons on $\epsilon_{2,l}$ rotate clockwise, while those on $\epsilon_{3,l}$ do anticlockwise. Namely, the almost complete or partial cancellation of the angular momentum can occur.

interactions, the TLL parameter $K_{0,s,a}$ are known to be larger than unity. [9] The vertex term $\cos(2\theta_0 - 2\theta_s)$ thus must be strongly relevant [14] and $\theta_0 - \theta_s$ is locked at $\pi/2$, which is consistent with our previous result (10d). Introducing new fields $(\varphi_{\pm}, \theta_{\pm}) = (\varphi_0 \pm \varphi_s, \theta_0 \pm \theta_s)/\sqrt{2}$, we can interpret that the cosine term opens a gap in the (φ_-, θ_-) sector. Following the method in Ref. [20], we can trace out the degrees of freedom of the gapped sector. After that, we finally obtain a two-component TLL Hamiltonian with the (φ_+, θ_+) and (φ_a, θ_a) sectors as the low-energy effective theory.

On the other hand, when $\bar{\rho}_a$ is too large in Eq. (13), we should adopt $(\bar{\rho}_1, \bar{\rho}_{-1}) = (\bar{\rho}_s, 0)$ or $(0, \bar{\rho}_s)$ as the proper GL solution instead of Eq. (13). For this case, neglecting all of the parts with the field ϕ_{-1} in the Hamiltonian (8), we again derive a two-component TLL Hamiltonian.

Consequently, we conclude from the second analysis above that the ground state possesses a finite angular momentum $\bar{\rho}_a \neq 0$ and the low-energy excitations are described by a two-component TLL. [21]

V. SUMMARY AND DISCUSSIONS

In this paper, we have studied the 1D harmonically trapped Bose gas (1) with bosons on multi-transverse modes. Starting from the 3D boson systems with 2D confinement potential, the 1D effective Hamiltonian is derived by integrating out the degrees of freedom of all the vacant bands. Applying two theoretical ways based on the GL approach and the bosonization to the 1D effective Hamiltonian (8), we have shown that when bosons are filled in the lower three bands under the conditions (3)-(5), an angular momentum becomes finite and the Z_2 reflection symmetry in the trapped plane is spontaneously broken. This phenomenon essentially originates from the larger repulsive interaction between the degenerate bands $(n, l) = (1, \pm 1)$ than the intraband repulsion. The second analysis in Sec. IV predicts that the low-energy excitations on the rotating ground state are described by a two-

component TLL. [21] It is known that when the bosons occupy only the lowest bands, the low-energy physics is governed by a one-component TLL. We thus can draw the phase diagram in Fig. 3.

The conjugate field for ρ_a is not realistic in the model (1). Any trigger of the rotating ground state therefore seems to be absent. However, the real trap potential must deviate from the harmonic type. Such a small deviation would help the system circulate clockwise or anticlockwise. Thermal fluctuations and large deformations of the trapped potential would generate kink structures between clockwise and anticlockwise rotating regimes. When Bose atoms carry an electric charge, the predicted rotation means spontaneous loop current and magnetic flux. If we suddenly change the form of the trap potential and then observe the real-space boson density profile, we can detect, in principle, whether the bosons rotate clockwise or anticlockwise.

APPENDIX A: SYMMETRY ARGUMENT

Here, we briefly summarized the symmetries of our Bose gas system (1). They are often used in our analyses of Secs. III and IV.

The Hamiltonian (1) is invariant under the following symmetry operations: The translation and the parity for the x -axis [$\psi(x, y, z) \rightarrow \psi(x + \delta, y, z)$ ($\delta \in \mathbf{R}$) and $\psi(x, y, z) \rightarrow \psi(-x, y, z)$], the Z_2 reflection and the SO(2) rotation in the y - z plane [$\psi(x, y, z) \rightarrow \psi(x, -y, z)$ and $\psi(\vec{r}) \rightarrow \psi(x, y \cos \Phi - z \sin \Phi, y \sin \Phi + z \cos \Phi)$ ($\Phi \in \mathbf{R}$)], and the global U(1) gauge transformation [$\psi(x, y, z) \rightarrow \psi(x, y, z)e^{i\Theta}$ ($\Theta \in \mathbf{R}$)].

For the bosonized phase-field Hamiltonians (e.g., Eq. (14)), it is important to note that all of the above symmetry operations can be translated to the bosonization language. [18] The translation and the parity operation for the x -direction, the Z_2 reflection and the SO(2) rotation in the y - z plane, and the global U(1) gauge transformation are, respectively, expressed as

$$[\varphi_{\alpha}(x), \theta_{\alpha}(x)] \rightarrow [\varphi_{\alpha}(x + \delta) + \pi\bar{\rho}_{\alpha}\delta, \theta_{\alpha}(x + \delta)], \quad (\text{A1a})$$

$$[\varphi_{\alpha}(x), \theta_{\alpha}(x)] \rightarrow [-\varphi_{\alpha}(-x), \theta_{\alpha}(-x)], \quad (\text{A1b})$$

$$[\varphi_{\alpha}(x), \theta_{\alpha}(x), \bar{\rho}_{\alpha}] \rightarrow [\varphi_{-\alpha}(x), \theta_{-\alpha}(x), \bar{\rho}_{-\alpha}], \quad (\text{A1c})$$

$$[\varphi_{\alpha}(x), \theta_{\alpha}(x)] \rightarrow [\varphi_{\alpha}(x), \theta_{\alpha}(x) - \alpha\Phi], \quad (\text{A1d})$$

$$[\varphi_{\alpha}(x), \theta_{\alpha}(x)] \rightarrow [\varphi_{\alpha}(x), \theta_{\alpha}(x) + \Theta], \quad (\text{A1e})$$

where $\alpha = 0, \pm 1$. Using another set of the phase fields $(\varphi_{s,a}, \theta_{s,a}) = (\varphi_1 \pm \varphi_{-1}, \frac{\theta_1 \pm \theta_{-1}}{2})$, we can further transform Eq. (A1) as

$$[\varphi_a(x), \theta_a(x)] \rightarrow [\varphi_a(x + \delta) + \pi\bar{\rho}_a\delta, \theta_a(x + \delta)], \quad (\text{A2a})$$

$$[\varphi_a(x), \theta_a(x)] \rightarrow [-\varphi_a(-x), \theta_a(-x)], \quad (\text{A2b})$$

$$[\varphi_a(x), \theta_a(x), \bar{\rho}_a] \rightarrow [-\varphi_a(x), -\theta_a(x), -\bar{\rho}_a], \quad (\text{A2c})$$

$$[\varphi_a(x), \theta_a(x)] \rightarrow [\varphi_a(x), \theta_a(x) - \Phi], \quad (\text{A2d})$$

$$[\varphi_a(x), \theta_a(x)] \rightarrow [\varphi_a(x), \theta_a(x)], \quad (\text{A2e})$$

for (φ_a, θ_a) , and

$$[\varphi_s(x), \theta_s(x)] \rightarrow [\theta_s(x + \delta), \varphi_s(x + \delta) + \pi \bar{\rho}_s \delta], \quad (\text{A3a})$$

$$[\varphi_s(x), \theta_s(x)] \rightarrow [-\varphi_s(-x), \theta_s(-x)], \quad (\text{A3b})$$

$$[\varphi_s(x), \theta_s(x)] \rightarrow [\varphi_s(x), \theta_s(x)], \quad (\text{A3c})$$

$$[\varphi_s(x), \theta_s(x)] \rightarrow [\varphi_s(x), \theta_s(x)], \quad (\text{A3d})$$

$$[\varphi_s(x), \theta_s(x)] \rightarrow [\varphi_s(x), \theta_s(x) + \Theta], \quad (\text{A3e})$$

for (φ_s, θ_s) . Note that $\bar{\rho}_a$ changes the sign under the Z_2 reflection in the y - z plane shown in Eq. (A2c).

For instance, applying these symmetries, we can

strongly restrict possible operators in the bosonized Hamiltonian (14).

ACKNOWLEDGMENTS

The authors are grateful to M. Cazalilla, K. Kamide, M. Ueda, A. Furusaki, and M. Oshikawa for useful discussions. A. T. was supported by JSPS and M. S. was supported by Grant-in-Aid for Scientific Research from MEXT (Grant No. 17071011).

-
- [1] A. J. Leggett, Rev. Mod. Phys. **73**, 307 (2001); *ibid.* **75**, 1083 (2003).
 - [2] C. J. Pethick and H. Smith, *Bose-Einstein Condensation in Dilute Gases* (Cambridge University Press, 2001);
 - [3] E. A. Cornell and C. E. Wieman, Rev. Mod. Phys. **74**, 875 (2002).
 - [4] L. Pitaevskii and S. Stringari, *Bose-Einstein Condensation* (Oxford University Press, 2003).
 - [5] J. Fortágh and C. Zimmermann, Rev. Mod. Phys. **79**, 235 (2007), and see the references therein.
 - [6] J. H. Thywissen, M. Olshanii, G. Zabow, M. Drndić, K. S. Johnson, R. M. Westervelt, and M. Prentiss, Eur. Phys. J. D **7**, 361 (1999).
 - [7] A. Görlitz, J. M. Vogels, A. E. Leanhardt, C. Raman, T. L. Gustavson, J. R. Abo-Shaeer, A. P. Chikkatur, S. Gupta, S. Inouye, T. Rosenband, and W. Ketterle, Phys. Rev. Lett. **87**, 130402 (2001).
 - [8] M. Olshanii, Phys. Rev. Lett. **81**, 938 (1998).
 - [9] M. A. Cazalilla, At. Mol. Opt. Phys. **37**, S1 (2004).
 - [10] M. Girardeau, J. Math. Phys. **1**, 516 (1960).
 - [11] T. Kinoshita, T. Wenger and D. S. Weiss, Science **305**, 1125 (2004); Phys. Rev. Lett. **95**, 190406 (2005).
 - [12] B. Paredes, A. Widera, V. Murg, O. Mandel, S. Fölling, I. Cirac, G. V. Shlyapnikov, T. W. Hänsch, and I. Bloch, Nature (London) **429**, 277 (2004).
 - [13] F. D. M. Haldane, Phys. Rev. Lett. **47**, 1840 (1981); *ibid.* **48**, 569 (1982).
 - [14] T. Giamarchi, *Quantum Physics in One Dimension* (Oxford University Press, 2004).
 - [15] K. Yang, Phys. Rev. Lett. **93**, 066401 (2004) and references therein.
 - [16] A. Kolezhuk and T. Vekua, Phys. Rev. B **72**, 094424 (2005).
 - [17] M. A. Cazalilla and A. F. Ho, Phys. Rev. Lett. **91**, 150403 (2003).
 - [18] M. Sato and T. Sakai, Phys. Rev. B **75**, 14411 (2007).
 - [19] Actually, $\Gamma_a^{(4)}$ is not always positive. If $\Gamma_a^{(4)}$ is negative, the further higher order correction is needed.
 - [20] L. Balents and M. P. A. Fisher, Phys. Rev. B **53**, 12133 (1996).
 - [21] If $\tilde{g}_{0s} \propto 4\tilde{\Gamma}_{01}$ is comparable with coefficients of $(\partial_x \varphi_{0,s})^2$ or $\bar{\rho}_a$ approaches $\bar{\rho}_s$ in Eq. (14), the low-energy excitation structure might qualitatively change. [15]